Conjugation with polyamines enhances the antitumor activity of naphthoquinones against human glioblastoma cells

Luciana Romão[a,b], Vanessa P. do Canto[c], Paulo A. Netz[c], Vivaldo Moura-Neto[b], Ângelo C. Pinto[d,✠] and Cristian Follmer[e]

Glioblastoma multiform (GBM) is the most common and devastating type of primary brain tumor, being considered the deadliest of human cancers. In this context, extensive efforts have been undertaken to develop new drugs that exhibit both antiproliferation and antimetastasis effects on GBM. 1,4-Naphthoquinone (1,4-NQ) scaffold has been found in compounds able to inhibit important biological targets associated with cancer, which includes DNA topoisomerase, Hsp90 and monoamine oxidase. Among potential antineoplastic 1,4-NQs is the plant-derived lapachol (2-hydroxy-3-prenyl-1,4-naphthoquinone) that was found to be active against the Walker-256 carcinoma and Yoshida sarcoma. In the present study, we examined the effect of polyamine (PA)-conjugated derivatives of lapachol, nor-lapachol and lawsone on the growth and invasion of the human GBM cells. The conjugation with PA (a spermidine analog) resulted in dose-dependent and time-dependent increase of cytotoxicity of the 1,4-NQs. In addition, in-vitro inhibition of GBM cell invasion by lapachol was increased upon PA conjugation. Previous biochemical experiments indicated that these PA-1,4-NQs are capable of inhibiting DNA human topoisomerase II-α (topo2α), a major enzyme involved in maintaining DNA topology. Herein, we applied molecular docking to investigate the binding of PA-1,4-NQs to the ATPase site of topo2α. The most active molecules preferentially bind at the ATP-binding site of topo2α, which is energetically favored by the conjugation with PA. Taken together, these findings suggested that the PA-1,4-NQ conjugates might represent potential molecules in the development of new drugs in chemotherapy for malignant brain tumors. *Anti-Cancer Drugs* **00:000–000**

Anti-Cancer Drugs 2018, **00**:000–000

Keywords: glioblastoma, lapachol, naphthoquinones, polyamine-conjugates, topoisomerase

[a]Campus Xerém, [b]Institute of Biomedical Sciences, [c]Institute of Chemistry, [d]Department of Organic Chemistry and [e]Department of Physical Chemistry, Institute of Chemistry, Federal University of Rio de Janeiro, Rio de Janeiro, Brazil

Correspondence to Cristian Follmer, PhD, Department of Physical Chemistry, Institute of Chemistry, Federal University of Rio de Janeiro, Rio de Janeiro 21941-909, Brazil
Tel: +55 21 2562 7752; fax: +55 21 2562 7265; e-mail: follmer@iq.ufrj.br

✠Deceased.

Received 6 November 2017 **Revised form accepted** 23 February 2018

Introduction

Glioblastoma multiform (GBM) are malignant tumors of the central nervous system, with a very weak response to current chemotherapies, notably because of a high level of intrinsic drug resistance [1]. In addition, this type of tumor is difficult to be removed surgically because of its tendency to diffusely invade the local brain [2]. The current standard treatment is based on maximal surgical resection, radiotherapy and administration of the drug temozolomide [3]. However, little success has been obtained in extending the life expectancy of patients diagnosed with GBM. As a result, this type of cancer is associated with a very poor prognosis, with a mean overall survival of 14 months [4]. In this context, the development of new therapeutic strategies to treat GBM requires the identification of compounds capable of inhibiting not only the tumor growth but also its ability of invasion.

Quinones have been associated with a broad range of biological properties, and many clinically important antineoplastic drugs, including anthracyclines, daunorubicin, mitomycin, mitoxantrones, doxorubicin and saintopin, display a quinone moiety [5,6]. 1,4-Naphthoquinone (1,4-NQ) in particular is found in many inhibitors of biological targets associated with cancer, which include DNA topoisomerase [7], Hsp90 [8] and monoamine oxidase (MAO) [9]. Among plant-derived 1,4-NQs with potential anticancer properties are lapachol, a compound isolated from the tree *Tabebuia avellandedae*, plumbagin, shikonin and juglone. These molecules exhibit cytotoxic activities against different types of tumor including carcinomas, sarcomas, breast cancer, melanoma, pancreatic cancer, and prostate cancer [10–13]. Vitamin K is also a group of biologically active 1,4-NQs that is believed to have important anticancer properties [14].

A possible strategy to enhance the antineoplastic activity of chemotherapeutic agents is based on the conjugation of these molecules with a polyamine (PA) backbone [15,16]. The conjugation with PA may be an effective way of selectively delivering cytotoxic molecules into

Supplemental Digital Content is available for this article. Direct URL citations appear in the printed text and are provided in the HTML and PDF versions of this article on the journal's website, www.anti-cancerdrugs.com.

DOI: 10.1097/CAD.0000000000000619

human cancer cells by exploiting the highly active PA transporters in tumors [17]. In addition, PA moiety offers additional binding sites to the antitumor agents. For instance, PA might recognize the ionic surface of mitochondria and penetrate these organelles, an important property for drugs targeting cancer [18]. Using this approach, antitumor activities of 2-spermidine-3-R-1,4-NQs were demonstrated for cancer cell lines such as human promyelocytic leukemia, lung cancer, Burkitt lymphoma, and mouse breast tumor [16]. The antitumor activity of spermidine-1,4-NQs is attributed to the inhibition of DNA human topoisomerase II-α (topo2α), an enzyme involved in maintaining DNA topology, as demonstrated by biochemical assays using purified ATPase domain of topo2α [19].

In the present work, we investigate the anticancer properties of a series of PA-1,4-NQ conjugates against two lines of GBM cells: U87MG and GBM95. These molecules exhibit a 1,4-NQ scaffold linked with a spermidine analog. Our results show that the conjugation with PA enhanced the antitumor activity of lapachol, lawsone and nor-lapachol against GBM cells. In addition, the attachment to PA significantly improved the ability of 1,4-NQs in inhibiting tumor invasion *in vitro*. By using molecular docking tools, we demonstrated that the conjugation with PA favored the interaction of 1,4-NQs with ATP-binding site of topo2α. Collectively, our findings suggest that PA-1,4-NQs are promising antitumor agents against malignant brain tumors.

Methods

Synthesis of spermidine-1,4-naphthoquinone

Spermidine-1,4-NQs were synthesized and characterized as described by Cunha *et al.* [19] and Coelho-Cerqueira *et al.* [9] The synthesis steps are indicated in Fig. 1, in which PA (spermidine analog) was conjugated to lapachol (**a**), lawsone (**b**) or nor-lapachol (**c**). The steps of the synthesis were as follows: (i) the methylation of **a** and **c** with dimethylsulphate in acetone and potassium carbonate to yield **1a** and **1c**, and synthesis of methoxylawsone (**1b**) from the sodium salt of 1,2-naphthoquinone-4-sulfonic acid; (ii) preparation of the protected derivative of spermidine, **2**; (iii) nucleophilic displacement of the methoxyquinones **1a**, **1b**, and **1c** with **2**, to yield the compounds **3a**, **3b** and **3c** (Fig. 1). To remove the protecting group BOC from 3b, a solution of TFA (0.20 ml; 2.6 mmol) in CH_2Cl_2 (5 ml) was slowly added to a solution of **3b** (62.7 mg; 0.13 mmol) in methanol (20 ml) at 0°C. After 10 min, the reaction was taken to room temperature and kept under stirring for 4 h until total consumption of the starting material. The solvent was removed under reduced pressure; addition of 10% $KHCO_3$ (10 ml) was followed by extraction with CH_2Cl_2. The organic phase was dried with anhydrous Na_2SO_4 and concentrated under reduced pressure to give the free amine, **4b** (50.3 mg, 99%), as a red oil that was purified by flash chromatography (ethyl acetate/methanol, 6 : 4) [$R_f = 0.2$ (CH_2Cl_2/methanol/triethylamine 10 : 89 : 1)]. A similar procedure was followed for the syntheses of

Fig. 1

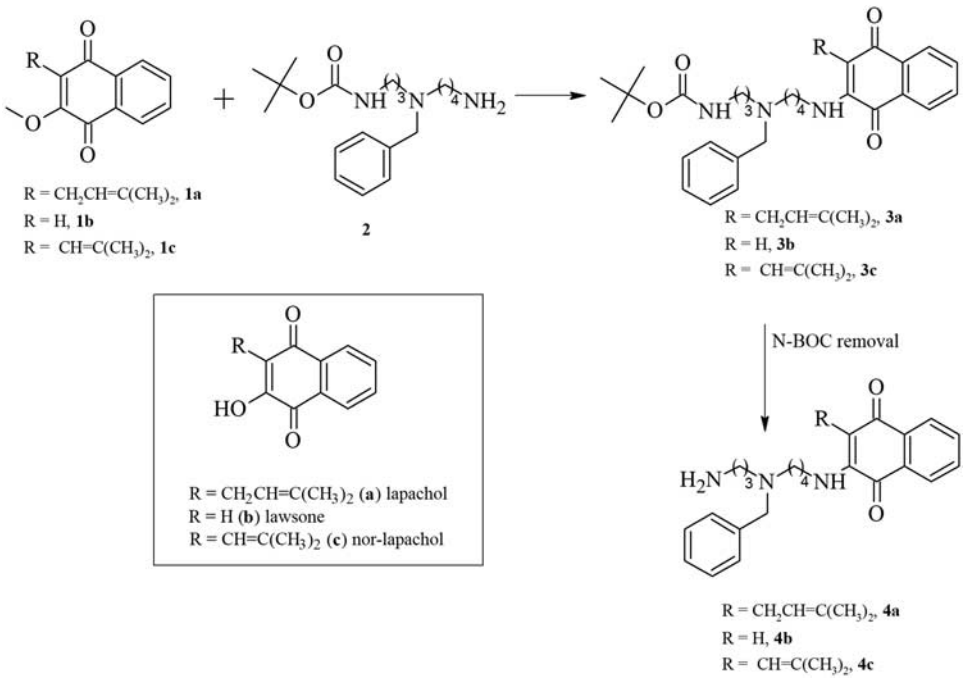

Steps of the synthesis of PA-1,4-NQ conjugates. 1,4-NQs, 1,4-naphthoquinone; PA, polyamine.

compounds **4a** and **4c**, which were purified as mentioned above using ethyl acetate/methanol 6 : 4 as eluent and obtained as a brown reddish oil (57.9 mg, 97%) [R_f = 0.2 (CH_2Cl_2/methanol/triethylamine 10 : 89 : 1)]. Characterization of all the compounds by MS, FTIR and NMR was previously described by our group [9].

Astrocyte primary cultures

Astrocyte primary cultures were prepared from the cerebral cortex of newborn mice as previously described [20]. Briefly, single-cell suspensions were obtained by dissociating cells from the cerebral cortex in a medium consisting of Dulbecco's minimum essential medium (DMEM) and nutrient mixture F12 (DMEM/F12; Invitrogen, Carlsbad, California, USA), enriched with glucose (33 mmol/l), glutamine (2 mmol/l) and sodium bicarbonate (30 mmol/l). The cells were plated in dishes or onto coverslips treated with poly-L-ornithine (Sigma-Aldrich Co., St. Louis, Missouri, USA) and maintained in DMEM/F12 medium supplemented with 10% fetal bovine serum (Invitrogen). The cultures were incubated at 37°C in humidified 5% CO_2 and 95% air atmosphere. The medium was changed every 2 days until the cells reached confluence. The astrocyte primary cultures were assessed by immunocytochemistry, using an antiglial fibrillary acidic protein antibody, and cells presented more than 95% purity.

Maintenance of the GBM cell lines

The human GBM cell line (GBM95) was obtained according to Faria *et al.* [21], following procedures established by the Brazilian Ministry of Health Ethic Committee (CONEP no. 2340). The GBM95 cell lines were derived from human samples and obtained with consent from the Brazilian Ministry of Health Ethic Committee and with consent from the patients in the form of written statements. The cell lines were grown and maintained in DMEM/F12 supplemented with 10% (v/v) fetal bovine serum. The culture flasks were maintained at 37°C in 5% CO_2 and 95% air. Cells displaying exponential growth were detached from the culture flasks with 0.25% trypsin/EDTA, and they were seeded at different densities, depending on the assay. The U87MG cell line was obtained from the American Type Culture Collection (Manassas, Virginia, USA).

3-(4,5-Dimethylthiazol-2-yl)-2,5-diphenyltetrazolium bromide cytotoxicity assay

GBM95 and U87MG tumor cell lines and mouse astrocyte cell cultures were seeded (3×10^4 cells/well) with 10% FBS DMEM-F12 medium in 96-well culture plates and cultured for 24 h. The cells were treated with 10, 25, 50 and 100 µmol/l of lapachol (**a**), lawsone (**b**), nor-lapachol (**c**), or their PA-conjugate derivatives (**3a**, **3b**, **3c**, **4a**, **4b**, and **4c**) for 24, 48 or 72 h. Viable cells were quantified by the 3-(4,5-dimethylthiazol-2-yl)-2,5-diphenyltetrazolium bromide cytotoxicity assay, as previously described [22]. The cell survival fraction was measured at each drug concentration as the ratio of absorbance at 560 nm, relative to vehicle-treated cells.

Tumor invasion assay

For formation of the spheroids, a single-cell suspension was generated from trypsinized monolayers and diluted at the desired cell density, and the suspension was mixed in DMEM/10% FBS. Spheroids were formed using the well-known hanging drop method (25 µl, 2000 cells per sphere). Spherical organization of spheroids/condition was followed regularly from 0 to 72 h on phase-contrast images (Nikon TE 2000 inverted microscope, Nikon Instruments Inc., Melville, New York, USA). Area measurements were measured using shape descriptors of ImageJ software (*https://imagej.nih.gov/ij/*). For spheroid invasion assays, the 3D component of the system consisted of a collagen gel matrix, prepared immediately before the spheroid culture, using a 4 : 1 mixture of purified bovine collagen I and DMEM with 1.0 mol/l NaOH, as necessary for neutralization of the mixture [23]. For each experiment, 50 µl of this neutralized solution was pipetted into each well of a 96-well plate and placed into a 37°C, humidified incubator for 1 h to induce gelation. One spheroid was added to the surface of each gel using forceps, and the medium with the treatments was added. The spheroids were treated with 25 and 50 µmol/l of **a**, **3a**, **3b**, and **4a**, and the area was analyzed for 24, 48, and 72 h. The capacity of tumor invasion was measured through the area of the GBM95 cell spheroids (μm^2) after 24, 48 or 72 h, normalized to the area at the initial time (0 h).

Molecular docking

The structures of lapachol, lawsone, nor-lapachol, the spermidine-1,4-NQs (**3a**, **3b**, **3c**, **4a**, **4b**, and **4c**) and nucleotides ATP, ADP and ANP were built with GaussView 4.1 [24] and optimized with RHF/6-31G(d,p) using GAUSSIAN 09 [25]. Using AutoDock Tools [26], the nonpolar hydrogen atoms were merged to the heavy atoms. Gasteiger–Marsili partial charges were assigned as described [27], and the final structures of ligands were written as pdbqt files for further use in docking with AutoDock Vina [28].

The topo2α receptor structure was built as a modification of a structure obtained from the Protein Data Bank (PDB ID: 1ZXN). As described in the text, the topo2α receptor structure with AMP-PNP ligand (PDB ID: 1ZXM) was also built with the same procedure and used for structural comparison. These structures are ATPase domains of human DNA topo2α bound to ADP [29]. For docking purposes, both chain A and B were considered as the starting point. The grid box was built with $48 \times 48 \times 48$ points and constituted a large region surrounding the ATPase site of chain A and B. All dockings, using AutoDock Vina, were carried out in triplicate. The

interactions between the ligand and protein residues were analyzed with AutoDock Tools and Ligplot [30].

Results and Discussion

Conjugation with polyamine increases the antitumor activity of 1,4-naphthoquinones

GBM cells are remarkably resistant to radio and chemotherapies, and the current treatment still has poor outcomes; thereby, the efficient inhibition of both cell growth and tumor invasion is one of the major targets in GBM research. In the present study, we set out to investigate the effect of 1,4-NQs lapachol (**a**), lawsone (**b**) and nor-lapachol (**c**), and their PA-conjugate derivatives on the growth of GBM95 cell line. Figure 2a shows the cell viability, measured by 3-(4,5-dimethylthiazol-2-yl)-2,5-diphenyltetrazolium bromide assay, after incubation for 24 h. Lapachol and lawsone at 100 µmol/l exhibited a significant decrease in GBM95 cell viability (30–40%), without any observable toxicity on astrocyte cells. Nor-lapachol was ineffective at this concentration. Interestingly, the conjugation of these molecules with a spermidine analog significantly increased the toxicity of all 1,4-NQs. For **4a**, **3b**, **4b** and **3c,** the GBM cell viability is reduced in ~80%. In addition, the anticancer activity for the most active molecules occurred in a concentration-dependent manner (Fig. 2b and c). **4b** exhibited a poor specificity for tumor cells, affecting similarly GBM95 and astrocyte cells. For the other PA-conjugates, the gain in toxic activity fostered by PA conjugation was selective for GBM95 cells, being not observed on astrocytes. We can also note that the removal of the protecting group BOC from the PA backbone has controversial effects on the antitumor properties. For instance, removal of the BOC group from **3c** (providing **4c**) negatively affected the activity of this molecule, whereas an opposite effect was observed for PA-lapachol conjugates. The explanation for this inconsistent effect of the BOC group on the activities of PA-1,4-NQs is unclear. However, in most of the cases, the presence of the protecting group has a less significant impact on the antitumor action of these molecules than the conjugation with PA.

Next, we investigated the time dependence of the antitumor action against GBM cell lines and astrocyte cells using a lower concentration of PA-1,4-NQs (25 µmol/l). The toxicity of lapachol, lawsone and their PA-conjugates on GBM95 cells increased in a time-dependent manner

Fig. 2

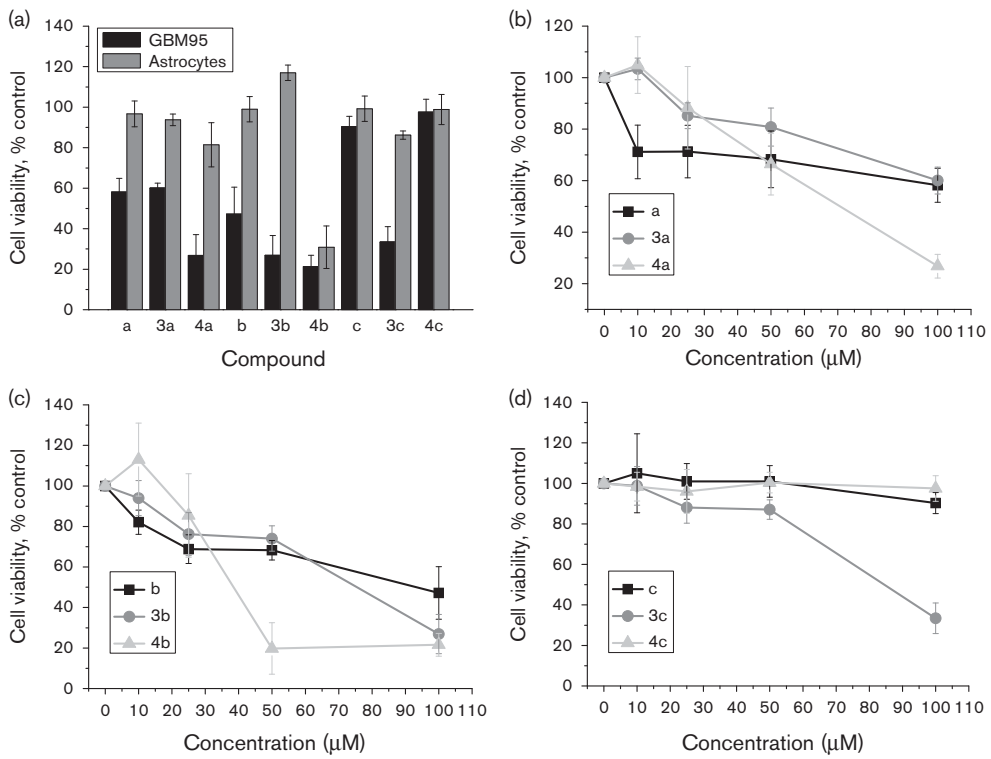

Effect of 1,4-NQs and their PA-conjugates on the viability of GBM95 and astrocyte cells. (a) Toxicity of 100 µmol/l of the compounds, measured by 3-(4,5-dimethylthiazol-2-yl)-2,5-diphenyltetrazolium bromide assay, on cell viability after 24 h of incubation. Concentration-dependent effect of the compounds **a** (lapachol), **3a** and **4a** (b), **b** (lawsone), **3b** and **4b** (c) or **c** (nor-lapachol), **3c** and **4c** (d) on the viability of GBM95 after 24 h of treatment. Toxicity assays were performed in triplicate, and the results are expressed as arithmetic mean ± SEM. 1,4-NQs, 1,4-naphthoquinone; PA, polyamine.

Fig. 3

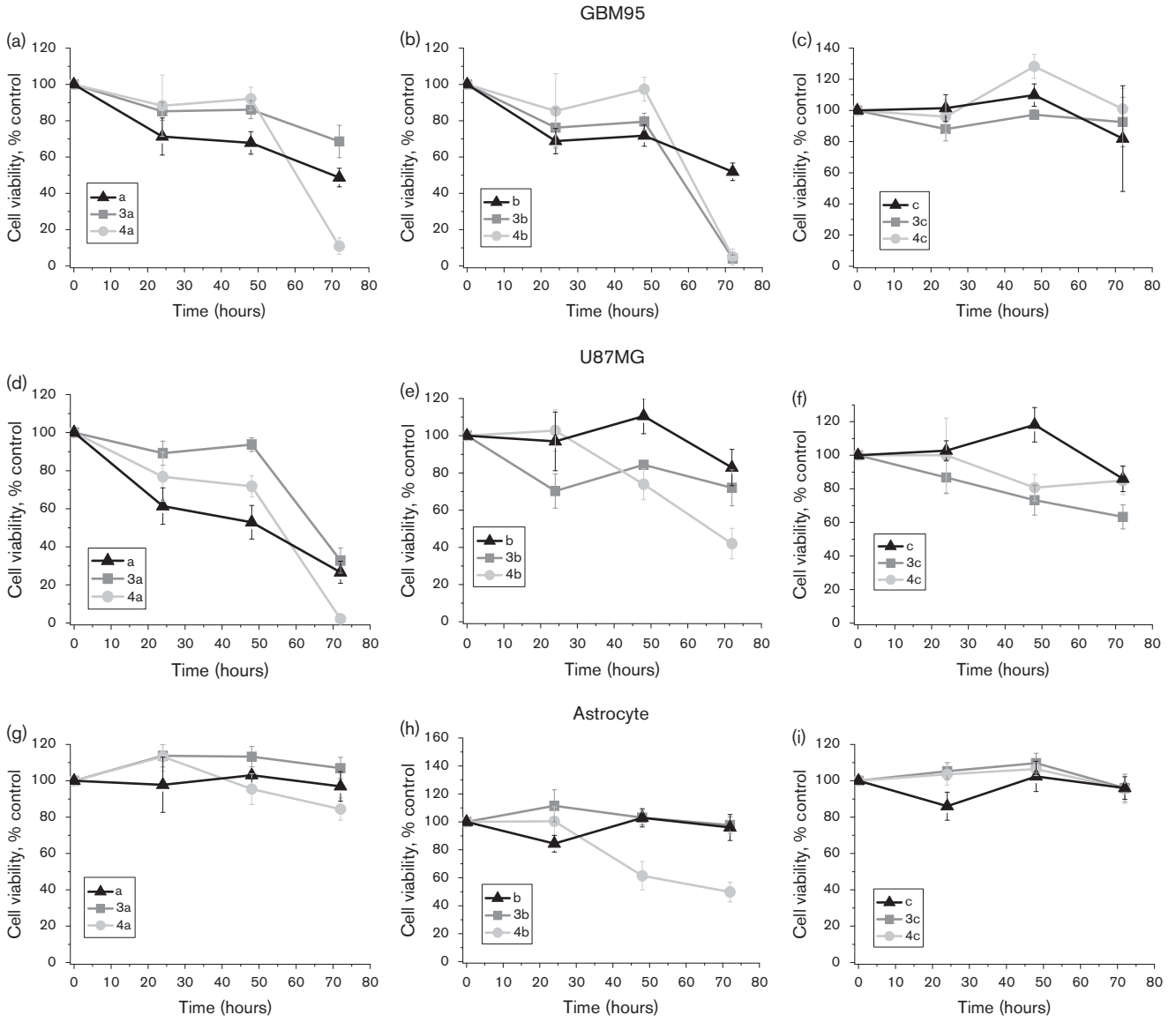

Antitumor activity of 1,4-NQs and their PA-conjugates occurs in a time-dependent manner. The cell lines, GBM95 (a–c) and U87MG (d–f), and astrocytes (g–i) were incubated in the presence of 25 μmol/l of each compound and the cell viability monitored over time. Toxicity assays were performed in triplicate, and the results are expressed as arithmetic mean ± SEM. 1,4-NQs, 1,4-naphthoquinone; PA, polyamine.

for most of the compounds (Fig. 3a and b). The attachment of PA seems to not increase the toxicity of nor-lapachol at 25 μmol/l, even after 72 h of incubation (Fig. 3c). The time-dependent toxicity was also evaluated using the U87MG, a commonly studied grade IV GBM-astrocytoma cell line, derived from human malignant glioma. In this case, U87MG seems to be slightly more sensitive than GBM95 to the toxic effects of lapachol (**a**), **3a** and **4a**, in which almost 100% of cell deaths was observed for this cell line after 72 h of treatment with **4a** (Fig. 3d). In contrast, U87MG was less susceptible to the PA-lawsone conjugates (**3b** and **4b**) than GBM95 (Fig. 3e). PA conjugation also increased the toxicity of the nor-lapachol derivative, **3c,** on U87MG (Fig. 3f). Collectively, these findings point out that lapachol and lawsone exhibit higher toxicity on GBM95 and U87MG cell lines than nor-lapachol, which is significantly increased by the conjugation with PA. In addition, PA conjugates **3a**, **4a** and **3b** display a higher specificity to GBM cells in comparison with astrocyte cells (Fig. 3g–i).

The half maximal inhibitory concentration (IC_{50}) values, after 72 h of incubation, were estimated for the most potent molecules, that is, lapachol, **3a**, **4a** and **3b**, using GBM95 and U87MG cell lines (Table 1). Although **3b**

potentially inhibited GBM95 cells with an IC_{50} value of 3.6 μmol/l, it displayed a poor inhibition on U87MG growth (34 μmol/l). **4a** was the only compound capable of efficiently inhibiting both GBM95 and U87MG with similar IC_{50} values for these cell lines (6.6 and 4.3 μmol/l, respectively).

Table 1 The IC_{50} (μmol/l) values for the most active compounds against GBM cell lines GBM95 and U87MG (72 h of incubation)

GBM	Lapachol	3a	4a	3b
GBM95	23.4 ± 4.8	33 ± 7.2	6.6 ± 2.6	3.6 ± 1.2
U87MG	18.4 ± 4.1	23.6 ± 4.3	4.3 ± 2.2	34 ± 11

The capacity of GBM95 cell invasion was measured through the relative growth of cell spheroids in a collagen I matrix, monitored for three days after their formation, in the presence of either DMSO or the compounds **a**, **3a**, **4a** and **3b** (Fig. 4). The effect on tumor invasion was evaluated only for the most promising compounds on the basis of the toxicity on GBM95 cells and tumor selectivity. The compound **4a** was excluded, because it displayed high toxicity against astrocytes. We can notice that DMSO-treated cells exhibit a remarkable increase in the area of invasive cells measured after 72 h of incubation (~60-fold in relation to the initial time) (Fig. 4b). Lapachol exhibited only a slight reduction in the tumor invasion in comparison with DMSO. In contrast, the

Fig. 4

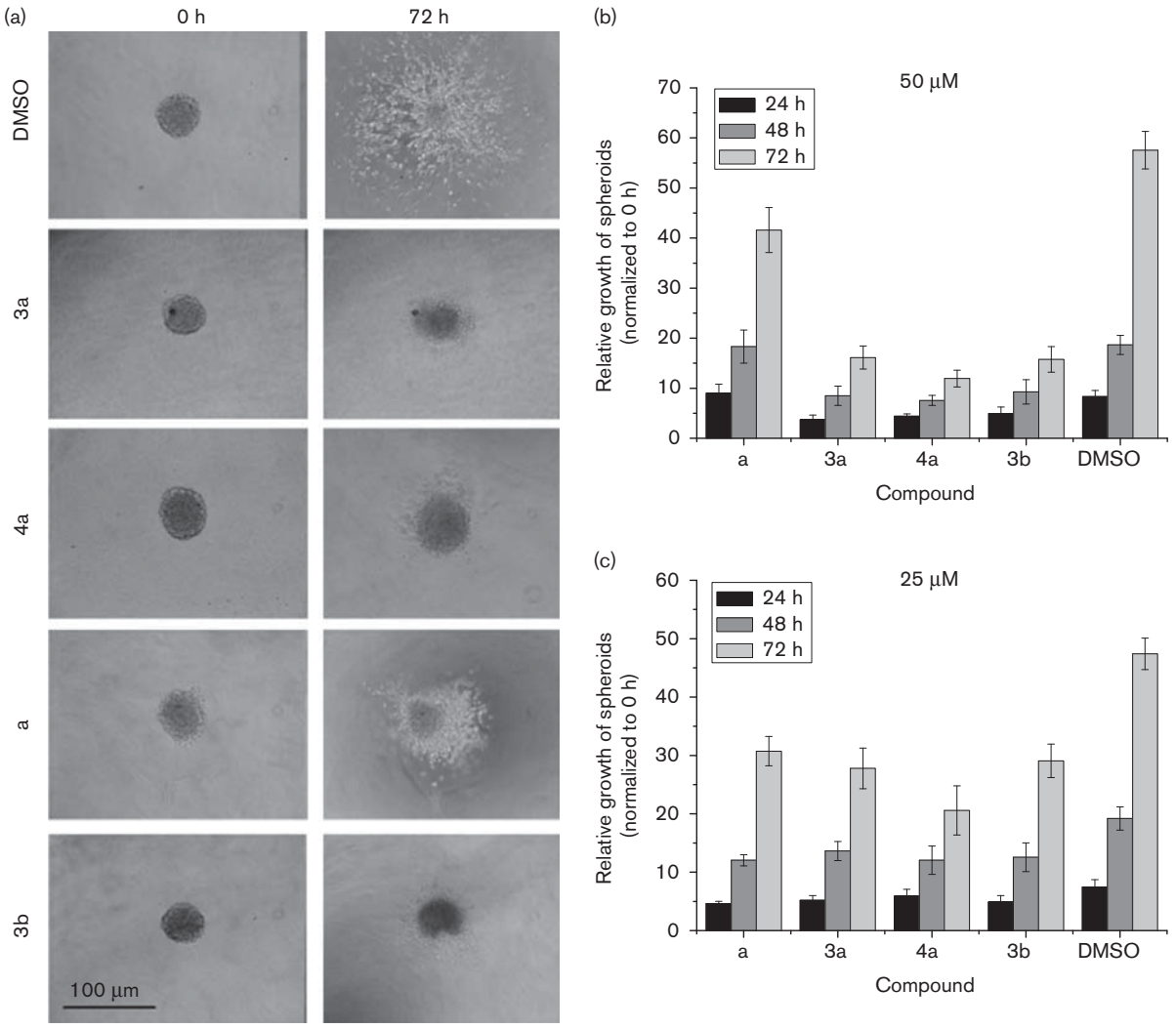

PA conjugation increases the inhibitory properties of 1,4-NQs on GBM95 cell invasion. (a) Growth of GBM95 cells as spheroids in culture at the initial time (0 h) or after 72 h of incubation with either DMSO or 50 μmol/l of the compounds **a**, **3a**, **4a** and **3b**. (b, c) show the relative growth of GBM95 spheroids after treatment with either 50 or 25 μmol/l of the compounds, respectively. DMSO alone was used as the control. Tumor invasion was measured through the area of the tumor spheroid (in μm^2) at a specific time normalized to the area at the initial time (0 h). The assays were performed in triplicate, and the results are expressed as arithmetic mean ± SEM. 1,4-NQs, 1,4-naphthoquinone; PA, polyamine.

Table 2 Binding energy (kcal/mol) of 1,4-naphthoquinones and their polyamine-conjugates into the ATPase site of topoisomerase II-α

Ligand	Free enzyme	Bound to ADP	ΔE[a]
a (lapachol)	−8.7[b]	−8.0[c]	
3a	−10.0[c]	−8.9[b]	−1.3
4a	−9.0[b]	−8.6[c]	−0.3
b (lawsone)	−7.9[b]	−6.8[c]	
3b	−10.3[c]	−8.9[c]	−2.4
4b	−9.5[b]	−8.2[c]	−1.6
c (nor-lapachol)	−8.7[b]	−7.9[c]	
3c	−10.4[c]	−8.2[c]	−1.7
4c	−9.0[c]	−8.9[c]	−0.3
ATP	−10.0[b]	−9.5[c]	
ADP	−10.0[b]	−8.7[c]	
AMP	−9.5[b]	−8.9[c]	

1,4-NQs, 1,4-naphthoquinone; PA, polyamine; topo2α, topoisomerase II-α.
[a]Change in the binding energy caused by PA attachment (free enzyme).
[b]Active site.
[c]Neighborhood of the active site, based on GBM95 cell line.

tumor invasion was significantly reduced by the presence of 50 μmol/l of the PA-conjugated **3a**, **4a** and **3b**. At a low concentration (25 μmol/l), PA conjugates and lapachol exhibited similar inhibitory activities on tumor invasion, which were still higher than the control (Fig. 4c).

PAs such as spermidine are present in high concentrations in rapidly proliferating cells [31]. PA analogues might work as potential vectors for the incorporation of chemotherapeutics into tumors, which might result in an increase of the selectivity and efficiency of the drug, either by facilitating uptake (through the active PA transporter), or by competition with PAs for 'critical binding sites' in the cells. In this context, an improvement of the activity of certain drugs such as antibiotics and anticancer agents upon PA conjugation has been reported by several studies [32–34]. For instance, antibacterial activity of chloramphenicol is enhanced when it is linked to PA, particularly against chloramphenicol-resistant strains. Chloramphenicol-PA conjugates also display an increased and more selective toxicity against human cancer cells [15]. The enhanced antitumor activity of PA-1,4-NQs observed in our studies might be attributed to a combination of diverse factors, which include an increase in the affinity for the already described cancer-related biological targets of 1,4-NQs.

Interaction of 1,4-naphthoquinones with the ATP-binding site of topoisomerase II-α is favored by polyamine conjugation

Previous biochemical experiments using the purified ATPase domain of topo2α revealed that 1,4-NQ is capable of inhibiting this enzyme [7]. In addition,relaxation assays using pBR322 supercoil DNA in the presence of ATP indicated that the, PA-1,4-NQs **3a**, **3b** and **3c** exhibit significant inhibition of topo2α catalytic activity, whereas PA alone did not have any effect [19]. Importantly, lapachol was able to only partially inhibit the enzyme even at a high concentration, which clearly demonstrates that the linkage of PA led to a remarkable increase in the capacity of lapachol in inhibiting topo2α. In contrast, none of the compounds were capable of inhibiting the enzyme, DNA-topo I [19].

To get further information on the mechanisms lying behind the antitumor activity of 1,4-NQ, we apply molecular docking to evaluate the binding site interactions of PA-1,4-NQs inside the human topo2α ATPase domain. For this purpose, we utilized the x-ray crystallography structure of dimeric enzyme with cocrystal ADP ligand as a reference molecule (PDB ID: 1ZXN). The binding energies for the best-docked conformations of the ligand with ATPase domain of topo2α are presented in Table 2. Lapachol, lawsone and nor-lapachol have binding energies with the free topo2α (without ADP) of -8.7, -7.9 and -8.7 kcal mol^{-1}, respectively, which are consistently more favorable (more negative energies) than those observed in the case of docking with the enzyme bound to ADP. In addition, the site of interaction with 1,4-NQs shifts to the neighborhood of the ATPase site when the enzyme is complexed with ADP. To verify whether lapachol occupies essentially the same position of ATP in the enzyme, the critical residues surrounding the ligands, ATP and lapachol, were investigated. When ATP is docked into the free enzyme, it interacts exactly in the same position of ADP (Supplementary Fig. 1SA, Supplemental digital content 1, *http://links.lww.com/ACD/A253*). Similar results were verified using as receptor topo2α with the cocrystal ligand AMP-PNP (a nonhydrolysable ATP analog) (PDB ID: 1ZXM) (Supplementary Fig. 1SB, Supplemental digital content 1, *http://links.lww.com/ACD/A253*). Lapachol docked into the free enzyme interacted with residues involved in ATP binding, which includes hydrogen bonds with Ser149, and Asn150 and van der Waals interactions with Tyr34, Asn91, Asn95, Ile125, Ser148, Gly161, Gly164, Gly166, Al3a67, Arg162 (Fig. 5a, b). The existence of additional residues participating in the ATP binding, that is, ATP has four more hydrogen bond than lapachol, could explain the more favorable binding energy observed for this ligand in comparison with lapachol (-10.0 kcal mol^{-1} for ATP against -8.7 kcal mol^{-1} for lapachol). Superposition of ATP and lapachol into the ATPase site indicates that these ligands compete essentially for the same binding site (Fig. 5d).

Afterwards, the effect of the attachment of PA to 1,4-NQs on the interaction with ATPase site of topo2α was addressed. For all 1,4-NQs, the linkage of PA favored the interaction with the enzyme, which might be attributed to the fact that the PA backbone provides additional interactions, with residues surrounding the ATPase binding site. The perturbation in the binding energy (ΔE) caused by PA conjugation is shown in Table 2. ΔE associated with the PA conjugation to **b** is considerably higher than that observed with the PA conjugation to **a**: -2.4 kcal mol^{-1} from **b** to **3b**; -1.3 kcal mol^{-1} from **a** to **3a**. Interestingly, the attachment of PA has a more

Fig. 5

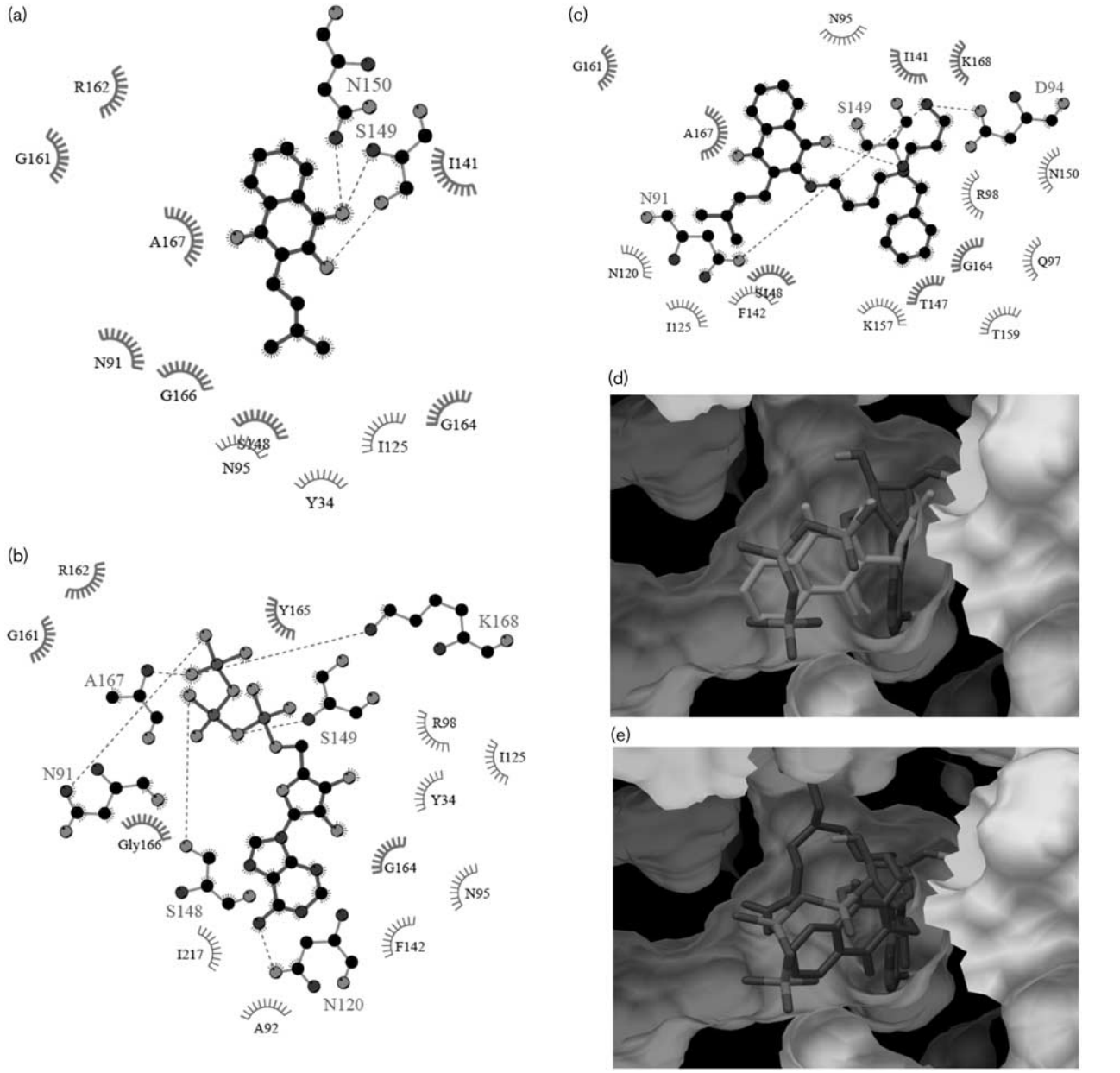

Molecular docking indicates that PA-1,4-NQs might act as topo2α inhibitors. Best-docked conformation of lapachol, ATP and **4a** into the ATPase site of topo2α are displayed in the (a–c), respectively. Superposition of ATP with lapachol (d) and ATP with **4a** (e) into the ATPase site indicates that these ligands compete essentially for the same binding site. 1,4-NQs, 1,4-naphthoquinone; PA, polyamine; topo2α, topoisomerase II-α.

significant influence on the antitumor activity of **b** than **a** (Fig. 3a vs. Fig. 3b). Despite **3a** exhibiting more favorable binding energy (-10.0 kcal mol^{-1}) than **4a**, the interaction of **3a** occurred at the neighborhood of the ATPase active site (Supplementary Fig. 2SA, Supplemental digital content 1, *http://links.lww.com/ACD/A253*). In contrast, **4a**, like lapachol, interacts at the ATPase site in the same position of ATP (Fig. 5e). Curiously, **3a** exhibits lower antitumor activity than **4a**. Similar results were obtained for lawsone derivatives. Like **3a**, **3b** interacts preferentially at the neighborhood ATP site (Supplementary Fig. 2SB, Supplemental digital content 1, *http://links.lww.com/ACD/A253*). However, **3a** and **3b** have opposite orientation to the ATPase site. The analysis of the superposition of ATP with either **3a** or **3b** into the ATP-binding site indicates that the 1,4-NQ ring of **3b** occupies a position very close to the adenine ring of ATP, whereas for **3a** the 1,4-NQ ring is far off the ATP site (Supplementary Fig. 2SC,D, Supplemental digital content 1, *http://links.lww.com/ACD/A253*). This could explain the

distinct activities of **3a** and **3b**. For nor-lapachol derivatives **3c** and **4c**, linkage to PA also favors the interaction at the neighborhood of the active site, and neither **3c** nor **4c** exhibited significant antitumor action on GBM95 or U87MG cell lines.

Topo2α is a homodimer enzyme that uses the energy of ATP hydrolysis to resolve topological problems that occur with the DNA during cell growth and division. A series of coordinated conformational changes regulates the binding and dissociation of ATP, whose hydrolysis regulates the opening and closing of molecular 'gates' that allow capture and restricting passage of duplex DNA [29]. Topo2α is a marker of cell proliferation and survival in GBM [35]. For instance, an increase in the expression of topo2α gene transcript have been reported in the GBM cell line U87MG [36]. In this context, inhibition of topo2α represents an important strategy in the design and development of new chemotherapy for GBM. The cellular consequence of such inhibition is an increase in the number of topo2α-DNA cleavage complexes entering into the cells, leading to apoptosis [37]. Our in-silico findings suggest that 1,4-NQs can bind to the ATPase site of topo2α, likely by occupying the ATP-binding site, which is favored by the conjugation with PA. In addition, a reasonable concordance was observed between the increased affinity for topo2α and the antitumor activity of PA-1,4-NQs.

Other possible targets of PA-1,4-NQ is the inhibition of MAO. MAO plays an important function not only in the process of cell growth and differentiation but also in the development and growth regulation of tumors. In addition, PAs such as spermidine are substrate for MAO and other amine oxidases [31,38]. In this context, diverse studies have suggested that MAO might be a promising target for cancer therapy. For instance, MAO-B activity is enhanced in malignant tumors in the central nervous system, and the degree of malignancy of astrocytoma has been positively correlated with the amine oxidase activity [39,40]. In addition, MAO-B inhibition by isatin results in apoptosis or necrosis of human neuroblastoma cells [41]. Previously, our group demonstrated that PA-1,4-NQ conjugates as well as 1,4-NQs themselves are potent MAO inhibitors [9]. These compounds inhibit MAO-A and MAO-B isoforms through a competitive mechanism: the enzyme selectivity is significantly affected by substitutions on the 1,4-NQ ring. Coincidently, **4a** and **4b** were also more potent inhibitors of MAO than lapachol or nor-lapachol. Although the main target of PA-1,4-NQs is likely the inhibition of topo2α, we cannot discard the hypothesis that the cytotoxic activity of these compounds on cancer cells might be, at least in part, influenced by their inhibitory action on MAO.

Conclusion

Our results indicate that PA conjugation is capable of improving the antitumor activity of 1,4-NQs against GBM cells. Previous biochemical assays as well as in-silico data collectively suggest that the main target of PA-1,4-NQs and 1,4-NQ themselves is the inhibition of topo2α. Although the exact reason why PA improves the antitumor action of 1,4-NQs is not totally elucidated, it likely involves a combination of factors that includes an enhanced selectivity and efficiency of the drug uptake into cells, as well as an increase in the affinity of 1,4-NQs for cancer-related biological targets such as topo2α and/or MAO.

Acknowledgements

This work was supported by Carlos Chagas Filho Foundation for Research Support of the State of Rio de Janeiro (FAPERJ) and National Counsel of Technological and Scientific Development (CNPq).

L.R. conducted most of the experiments. C.F. conceived the idea, analyzed the results and wrote the paper. V.P.C. and P.A.N. conducted the molecular docking analysis. V.M.N. participated in critically revising the manuscript.

Conflicts of interest

There are no conflicts of interest.

References

1 Lima FR, Kahn SA, Soletti RC, Biasoli D, Alves T, da Fonseca AC, *et al.* Glioblastoma: therapeutic challenges, what lies ahead. *Biochim Biophys Acta* 2012; **1826**:338–349.
2 Schiffer D, Cavalla P, Dutto A, Borsotti L. Cell proliferation and invasion in malignant gliomas. *Anticancer Res* 1997; **17**:61–69.
3 Stupp R, Mason WP, van den Bent MJ, Weller M, Fisher B, Taphoorn MJ, *et al.* Radiotherapy plus concomitant and adjuvant temozolomide for glioblastoma. *N Engl J Med* 2005; **352**:987–996.
4 Delgado-López PD, Corrales-García EM. Survival in glioblastoma: a review on the impact of treatment modalities. *Clin Transl Oncol* 2016; **18**:1062–1071.
5 Verma RP. Anti-cancer activities of 1,4-naphthoquinones: A QSAR study. *Anticancer Agents Med Chem* 2006; **6**:489–499.
6 Lu JJ, Bao JL, Wu GS, Xu WS, Huang MQ, Chen XP, *et al.* Quinones derived from plant secondary metabolites as anti-cancer agents. *Anticancer Agents Med Chem* 2013; **13**:456–463.
7 Gurbani D, Kukshal V, Laubenthal J, Kumar A, Pandey A, Tripathi S, *et al.* Mechanism of inhibition of the ATPase domain of human topoisomerase IIα by 1,4-benzoquinone, 1,2-naphthoquinone, 1,4-naphthoquinone, and 9,10-phenanthroquinone. *Toxicol Sci* 2012; **126**:372–390.
8 Hadden MK, Hill SA, Davenport J, Matts RL, Blagg BS. Synthesis and evaluation of Hsp90 inhibitors that contain 1,4-naphthoquinone scaffold. *Bioorg Med Chem* 2009; **17**:634–640.
9 Coelho-Cerqueira E, Netz PA, do Canto VP, Pinto AC, Follmer C. Beyond topoisomerase inhibition: antitumor 1,4-naphthoquinones as potential inhibitors of human monoamine oxidase. *Chem Biol Drug Des* 2014; **83**:401–410.
10 Balassiano IT, De Paulo SA, Henriques Silva N, Cabral MC, Carvalho MGC. Demonstration of the lapachol as a potential drug for reducing cancer metastasis. *Oncol Rep* 2005; **13**:329–333.
11 Panichayupakaranant P, Ahmad MI. Plumbagin and its role in chronic diseases. *Adv Exp Med Biol* 2016; **929**:229–246.
12 Yang JT, Li ZL, Wu JY, Lu FJ, Chen CH. An oxidative stress mechanism of shikonin in human glioma cells. *PLoS One* 2014; **9**:e94180.
13 Avcı E, Arıkoğlu H, Kaya DE. Investigation of juglone effects on metastasis and angiogenesis in pancreatic cancer cells. *Gene* 2016; **588**:74–78.
14 Jinghe X, Mizuta T, Ozaki I. Vitamin K and hepatocellular carcinoma: The basic and clinic. *World J Clin Cases* 2015; **3**:757–764.
15 Kostopoulou ON, Kouvela EC, Magoulas GE, Garnelis T, Panagoulias I, Rodi M, *et al.* Conjugation with polyamines enhances the antibacterial and anticancer activity of chloramphenicol. *Nucleic Acids Res* 2014; **42**:8621–8634.

16 Esteves-Souza A, Lucio KA, Cunha AS, Cunha Pinto A, Silva Lima EL, Camara CA, *et al*. Antitumoral activity of new polyamine-naphthoquinone conjugates. *Oncol Rep* 2008; **20**:225–231.
17 Wang C, Delcros JG, Cannon L, Konate F, Carias H, Biggerstaff J, *et al*. Defining the molecular requirements for the selective delivery of polyamine conjugates into cells containing active polyamine transporters. *J Med Chem* 2003; **46**:5129–5138.
18 Grancara S, Martinis P, Manente S, Garcia-Argaez AN, Tempera G, Bragadin M, *et al*. Bidirectional fluxes of spermine across the mitochondrial membrane. *Amino Acids* 2014; **46**:671–679.
19 Cunha AS, Lima ELS, Pinto AC, Esteves-Souza A, Echevarria A, Camara CA, Vargas MD, *et al*. Synthesis of novel naphthoquinone-spermidine conjugates and their effect on DNA topoisomerases I and II-α. *J Braz Chem Soc* 2006; **17**:439–442.
20 Romão LF, Sousa VO, Neto VM, Gomes FC. Glutamate activates GFAP gene promoter from cultured astrocytes through TGF-bet3a pathways. *J Neurochem* 2008; **2**:746–756.
21 Faria J, Romao L, Martins S, Alves T, Mendes FA, de Faria GP, *et al*. Interactive properties of human glioblastoma cells with brain neurons in culture and neuronal modulation of glial laminin organization. *Differentiation* 2006; **74**:562–572.
22 Gardner RS. A sensitive colorimetric assay for mitochondrial alpha-glycerophosphate dehydrogenase. *Anal Biochem* 1974; **59**:272–276.
23 Kofron CM, Fong VJ, Hoffman-Kim D. Neurite outgrowth at the interface of 2D and 3D growth environments. *J Neural Eng* 2009; **1**:016002.
24 Dennington R, Keith T, Millam J. *GaussView, Version 41*. Shawnee Mission, KS: Semichem Inc; 2007.
25 Frisch MJ, Trucks GW, Schlegel HB, Scuseria GE, Robb MA, Cheeseman JR, *et al*. *Gaussian 09, revision A1*. Wallingford, CT: Gaussian Inc.; 2013.
26 Sanner MF. Python: a programming language for software integration and development. *J Mol Graph Model* 1999; **17**:57–61.
27 Gasteiger J, Marsili M. Iterative partial equalization of orbital electronegativity – a rapid access to atomic charges. *Tetrahedron* 1980; **36**:3219–3228.
28 Trott O, Olson AJJ. Auto-DockVina: improving the speed and accuracy of docking with a new scoring function, efficient optimization, and multithreading. *Comput Chem* 2010; **31**:455–461.
29 Wie H, Ruthenburg AJ, Bechis SK, Verdine GL. Nucleotide-dependent domain movement in the ATPase domain of a human type IIA DNA topoisomerase. *J Biol Chem* 2005; **280**:37041–37047.
30 Wallace AC, Laskowski RA, Thornton JM. LIGPLOT: a program to generate schematic diagrams of protein-ligand interactions. *Protein Eng* 1996; **8**:127–134.
31 Agostinelli E, Arancia G, Vedova L, Belli F, Marra M, Salvi M, *et al*. The biological functions of polyamine oxidation products by amine oxidases: perspectives of clinical applications. *Amino Acids* 2004; **27**:347–358.
32 Kaur N, Delcros JG, Martin B, Phanstiel O 4th. Synthesis and biological evaluation of dihydromotuporamine derivatives in cells containing active polyamine transporters. *J Med Chem* 2005; **48**:3832–3839.
33 Delcros JG, Tomasi S, Duhieu S, Foucault M, Martin B, Le Roch M, *et al*. Effect of polyamine homologation on the transport and biological properties of heterocyclic amidines. *J Med Chem* 2006; **49**:232–245.
34 Phanstiel O 4th, Kaur N, Delcros JG. Structure-activity investigations of polyamine-anthracene conjugates and their uptake via the polyamine transporter. *Amino Acids* 2007; **33**:305–313.
35 Oda M, Arakawa Y, Kano H, Kawabata Y, Katsuki T, Shirahata M, *et al*. Quantitative analysis of topoisomerase IIalpha to rapidly evaluate cell proliferation in brain tumors. *Biochem Biophys Res Commun* 2005; **331**:971–976.
36 Hong Y, Sang M, Shang C, Xue YX, Liu YH. Quantitative analysis of topoisomerase II alpha and evaluation of its effects on cell proliferation and apoptosis in glioblastoma cancer stem cells. *Neurosci Lett* 2012; **518**:138–143.
37 Lu HR, Zhu H, Huang M, Chen Y, Cai YJ, Miao ZH, *et al*. Reactive oxygen species elicit apoptosis by concurrently disrupting topoisomerase II and DNA-dependent protein kinase. *Mol Pharmacol* 2005; **68**:983–994.
38 Toninello A, Salvi M, Mondov B. Interaction of biologically active amines with mitochondria and their role in the mitochondrial-mediated pathway of apoptosis. *Curr Med Chem* 2004; **11**:2349–2374.
39 Marcozzi G, Befani O, Mondov B. Type B monoamine oxidase activity in human brain malignant tumors. *Cancer Biochem Biophys* 1998; **16**:287–294.
40 Gabilondo AM, Hostalot C, Garibi JM, Meana JJ, Callado LF. Monoamine oxidase B activity is increased in human gliomas. *Neurochem Int* 2008; **52**:230–234.
41 Igosheva N, Lorz C, O'Conner E, Glover V, Mehmet H. Isatin, an endogenous monoamine oxidase inhibitor, triggers a dose- and time-dependent switch from apoptosis to necrosis in human neuroblastoma cells. *Neurochem Int* 2005; **47**:216–224.